

Exact distributions of the number of distinct and common sites visited by N independent random walkers

Anupam Kundu,¹ Satya N. Majumdar,¹ and Grégory Schehr¹

¹*Laboratoire de Physique Théorique et Modèles Statistiques (UMR 8626 du CNRS),
Université Paris-Sud, Bât. 100, 91405 Orsay Cedex, France*

We study the number of distinct sites $S_N(t)$ and common sites $W_N(t)$ visited by N independent one dimensional random walkers, all starting at the origin, after t time steps. We show that these two random variables can be mapped onto extreme value quantities associated to N independent random walkers. Using this mapping, we compute exactly their probability distributions $P_N^d(S, t)$ and $P_N^d(W, t)$ for any value of N in the limit of large time t , where the random walkers can be described by Brownian motions. In the large N limit one finds that $S_N(t)/\sqrt{t} \propto 2\sqrt{\log N} + \tilde{s}/(2\sqrt{\log N})$ and $W_N(t)/\sqrt{t} \propto \tilde{w}/N$ where \tilde{s} and \tilde{w} are random variables whose probability density functions (pdfs) are computed exactly and are found to be non trivial. We verify our results through direct numerical simulations.

PACS numbers: 05.40.-a, 02.50.-r, 05.40.Jc

In elementary set theory, two fundamental concepts are the *union* and the *intersection* of a number of N sets. While the union consists of all *distinct* elements of the collection of sets, the intersection consists of *common* elements of all the sets. These two notions appear naturally in everyday life: for example the area of common knowledge or the whole range of different interests amongst the members of a society would define respectively its stability and activity. In an habitat of N animals, the union of the territories covered by different animals sets the geographical range of the habitat, while the intersection refers to the common area (e. g. a water body) frequented by all animals.

In statistical physics, these two objects are modeled respectively by the number of distinct and common sites visited by N random walkers (RWs). The knowledge about the number of distinct sites has applications ranging from the annealing of defects in crystals [1, 2] and relaxation processes [3–6] to the spread of populations in ecology [7, 8] or to the dynamics of web annotation systems [9]. Similarly the knowledge about the common area frequented by endangered animals is very useful for their daily health caring. Likewise, in the energy transport through a series of independent disordered samples, the energy output will depend on the number of energy levels common to all these materials.

Dvoretzky and Erdős [10] first studied the average number of distinct sites $\langle S_1(t) \rangle$ visited by a single t -step RW in d -dimensions, subsequently studied in [11–13]. Larralde et al. generalized this to N independent, t -step walkers moving on a d -dimensional lattice [14]. They found three regimes of growth (early, intermediate and late) for the average number of distinct sites $\langle S_N(t) \rangle$ as a function of time. These three regimes are separated by two N -dependent times scales [14]. In particular they showed that in $d = 1$ and $t \gg \sqrt{\log N}$, $\langle S_N(t) \rangle \propto \sqrt{4D} t \log N$ where D is the diffusion constant of a single walker. Recently Majumdar and Tamm [15]

studied the complementary quantity, namely the number of common sites $W_N(t)$ visited by N walkers, each of t steps, and found analytically a rich asymptotic late time growth of the average $\langle W_N(t) \rangle$. They showed that in the $(N - d)$ plane there are three distinct phases separated by two critical lines $d = 2$ and $d_c(N) = 2N/(N - 1)$, with $\langle W_N(t) \rangle \sim t^\nu$ at late times where the growth exponent $\nu = d/2$ (for $d < 2$), $\nu = N - d(N - 1)/2$ [for $2 < d < d_c(N)$] and $\nu = 0$ [for $d > d_c(N)$] (see also [16]). In particular, in $d = 1$, $\langle W_N(t) \rangle \sim \sqrt{4Dt}$ where the prefactor depends on N . However, most of these studies were limited to the *average* number of distinct or common sites, and there exists virtually no information about their full probability distributions, e.g. the probabilities $P_N^d(S, t)$ that $S_N(t) = S$ and $P_N^c(W, t)$ that $W_N(t) = W$.

Computing these distributions for general d -dimensional space is highly non trivial. Indeed, although the N walkers are independent, conditioning their trajectories to a given number of distinct (or common) visited sites introduces strong effective correlations between them. In $d = 1$, we show here that these random variables $S_N(t)$ and $W_N(t)$ can be mapped onto extreme values (nearest and furthest displacements) associated to N independent walkers. This connection to extreme value statistics (EVS) allows us to compute $P_N^d(S, t)$ and $P_N^c(W, t)$ exactly for t large and arbitrary N . We show that the induced correlations between the walkers persist even for $N \rightarrow \infty$ where the limiting distributions are not given by EVS of independent random variables, as erroneously argued in the previous study of $S_N(t)$ [14].

We consider N independent and identical t -step RWs $x_1(\tau), x_2(\tau), \dots, x_N(\tau)$ on a $1-d$ lattice, all starting at the origin. For convenience, we set the diffusion constant of the walkers $D = \frac{1}{2}$. Distinct sites are those that are visited at least once by at least one of the N walkers [14], while common sites correspond to sites visited individually at least once by all the N walkers [15]. We denote by M_i and m_i respectively the maximum and the min-

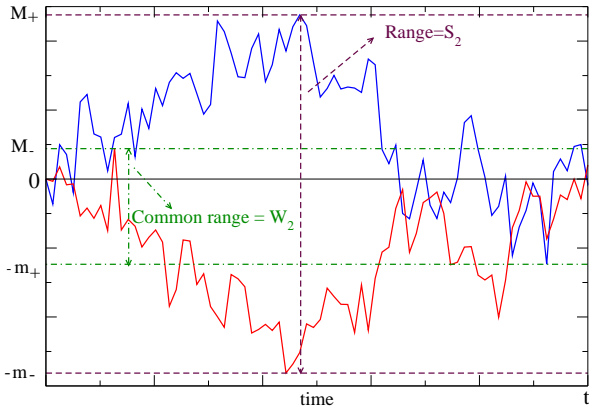


FIG. 1. (Color Online) Schematic diagram of 2 independent RWs, where M_+ , M_- , m_+ , m_- and S_2 , W_2 are shown (1, 2).

imum displacements of the i^{th} walker x_i up to time t . The number of distinct sites visited, S_N [17], is then the sum of the range on the positive (+ve) side, M_+ , and the range on the negative (-ve) side m_- (see Fig. 1):

$$S_N = M_+ + m_-, \quad M_+ = \max_{1 \leq i \leq N} M_i, \quad m_- = - \min_{1 \leq i \leq N} m_i. \quad (1)$$

Similarly, the number of common sites visited, W_N , is the common span on the +ve axis plus the common span m_+ on the -ve axis:

$$W_N = M_- + m_+, \quad M_- = \min_{1 \leq i \leq N} M_i, \quad m_+ = - \max_{1 \leq i \leq N} m_i. \quad (2)$$

Eqs. (1) and (2) establish a precise connection between S_N and W_N and the EVS of N independent RW's.

In the limit of large t , the lattice RWs converge to Brownian motions (BMs). Hence for large t , the probability distributions $P_N^d(S, t)$ and $P_N^c(W, t)$ take the scaling form

$$P_N^d(S, t) = \frac{1}{\sqrt{2t}} p_N^d \left(\frac{S}{\sqrt{2t}} \right), \quad P_N^c(W, t) = \frac{1}{\sqrt{2t}} p_N^c \left(\frac{W}{\sqrt{2t}} \right) \quad (3)$$

where $p_N^d(s)$ is the probability density function (pdf) of the span or range, $s = S/\sqrt{2t}$, and $p_N^c(w)$ is the pdf of the common span or common range, $w = W/\sqrt{2t}$, for N independent BMs (see Fig. 1) on the unit time interval [18]. The rescaled quantities $S_N/\sqrt{2t}$ and $W_N/\sqrt{2t}$ in (3) are given by (1) and (2) where M_{\pm}, m_{\pm} are replaced by their counterparts $\tilde{M}_{\pm} = M_{\pm}/\sqrt{2t}$ and $\tilde{m}_{\pm} = m_{\pm}/\sqrt{2t}$ corresponding to N independent BMs on the unit time interval.

It is useful to summarize our main results. We obtain exactly, for any N , the pdfs $p_N^d(s)$ and $p_N^c(w)$ as presented in (12) and (15) along with (8) and (9). The moments can also be computed explicitly [19]. The tails

of the pdfs can be derived explicitly:

$$p_N^d(s) \sim \begin{cases} a_N s^{-5} \exp[-N\pi^2/(4s^2)], & s \rightarrow 0, \\ b_N \exp(-s^2/2), & s \rightarrow \infty, \end{cases} \quad (4)$$

and

$$p_N^c(w) \sim \begin{cases} c_N w, & w \rightarrow 0 \\ d_N w^{1-N} \exp(-Nw^2), & w \rightarrow \infty, \end{cases} \quad (5)$$

where a_N, b_N, c_N and d_N are computable constants (see below). For $N \rightarrow \infty$, one finds that both pdfs approach a non trivial limiting form

$$p_N^d(s) \sim 2\sqrt{\log N} \mathcal{D} \left(2\sqrt{\log N} \left(s - 2\sqrt{\log N} \right) \right), \quad \mathcal{D}(\tilde{s}) = 2 e^{-\tilde{s}} K_0(2 e^{-\tilde{s}/2}), \quad (6)$$

where $K_n(x)$ denote the modified Bessel functions, and

$$p_N^c(w) = N \mathcal{C}(Nw), \quad \mathcal{C}(\tilde{w}) = \frac{4}{\pi} \tilde{w} e^{-\frac{2}{\sqrt{\pi}} \tilde{w}}, \quad \tilde{w} > 0. \quad (7)$$

Note that $\mathcal{D}(\tilde{s})$ (6) is not the Gumbel distribution, as it was initially argued in [14]. Remarkably the same distribution $\mathcal{D}(\tilde{s})$ also appears as the limiting distribution of the maximum of a large collection of logarithmically correlated random variables on a circle [20]. We check indeed $\int_{-\infty}^{\tilde{s}} \mathcal{D}(\tilde{s}') d\tilde{s}' = 2e^{-\tilde{s}/2} K_1(2e^{-\tilde{s}/2})$, as obtained in [20]. Incidentally, logarithmically correlated random variables have been the subject of several recent studies [20–22] because they exhibit freezing phenomena, akin to the replica symmetry breaking scenario found in mean field spin glass models [23]. As a byproduct of our computation, we show that $\mathcal{D}(\tilde{s})$ is the convolution of two independent Gumbel distributions.

We start by computing the joint cumulative distribution functions (jcdf) $\mathbf{P}_d(l_1, l_2) = \text{Pr}(\tilde{M}_+ \leq l_1, \tilde{m}_- \leq l_2)$, relevant for $p_N^d(s)$ and the jcdf $\mathbf{P}_c(j_1, j_2) = \text{Pr}(\tilde{M}_- \geq j_1, \tilde{m}_+ \geq j_2)$ relevant for $p_N^c(w)$. Since all the N BMs are identical and independent, $\mathbf{P}_d(l_1, l_2) = g^N(l_1, l_2)$, where $g(l_1, l_2) = \text{Pr}(\tilde{M} \leq l_1, \tilde{m} \geq -l_2)$ is the jcdf of the maximum \tilde{M} and the minimum \tilde{m} for a *single* BM on the unit time interval. It can be computed by the standard method of images [24]:

$$g(l_1, l_2) = \frac{2}{\pi} \sum_{n=0}^{\infty} \frac{1}{n + \frac{1}{2}} \sin \left(\frac{(2n+1)\pi l_2}{l_1 + l_2} \right) e^{-\left(\frac{(n+\frac{1}{2})\pi}{l_1+l_2} \right)^2}. \quad (8)$$

Similarly, $\mathbf{P}_c(j_1, j_2) = h^N(j_1, j_2)$ where $h(j_1, j_2) = \text{Pr}(\tilde{M} \geq j_1, \tilde{m} \leq -j_2)$ reads:

$$h(j_1, j_2) = 1 - \text{erf}(j_1) - \text{erf}(j_2) + g(j_1, j_2), \quad (9)$$

where $\text{erf}(x) = (2/\sqrt{\pi}) \int_0^x e^{-y^2} dy$, $\text{erf}(j_1) = \text{Pr}(\tilde{M} \leq j_1)$ and $\text{erf}(j_2) = \text{Pr}(\tilde{m} \geq -j_2)$. From the joint pdf

$\frac{\partial^2 \mathbf{P}_d(l_1, l_2)}{\partial l_1 \partial l_2}$ and using (1), we obtain

$$p_N^d(s) = \int_0^\infty dl_1 \int_0^\infty dl_2 \delta(s - l_1 - l_2) \frac{\partial^2 g^N}{\partial l_1 \partial l_2}, \quad (10)$$

with $g \equiv g(l_1, l_2)$. Similarly, from the joint pdf $\frac{\partial^2 \mathbf{P}_c(j_1, j_2)}{\partial j_1 \partial j_2}$ and using (2) we obtain,

$$p_N^c(w) = \int_0^\infty dj_1 \int_0^\infty dj_2 \delta(w - j_1 - j_2) \frac{\partial^2 h^N}{\partial j_1 \partial j_2}, \quad (11)$$

with $h \equiv h(j_1, j_2)$. For small values of N , the double integrals in (10) and (11) can be performed explicitly and numerical simulations confirm these exact results [19]. Below we provide a physical interpretation of these formulas (10, 11) and perform, separately, their asymptotic analysis both for small and large arguments. We also analyze their limiting form for $N \rightarrow \infty$.

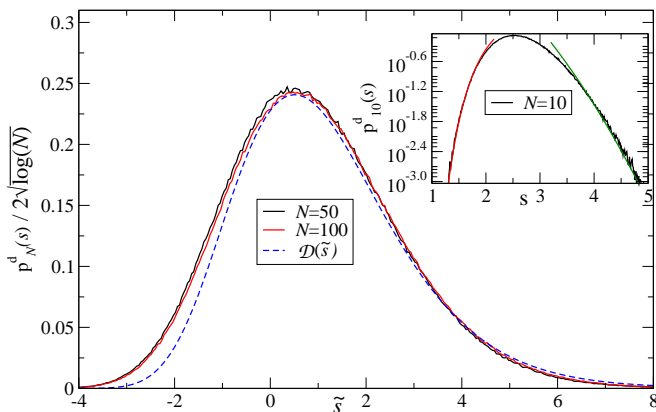


FIG. 2. (Color online) Plot of $p_N^d(s)/(2\sqrt{\log N})$ as a function of $\tilde{s} = 2\sqrt{\log N}(s - 2\sqrt{\log N})$. The dotted line indicates the exact asymptotic results for $N \rightarrow \infty$, $\mathcal{D}(\tilde{s})$ in (6). **Inset:** Plot of $p_{10}^d(s)$, obtained from simulation, compared with its asymptotic behavior (4).

Distinct sites : To find the tails of $p_N^d(s)$ at small and large s for finite N , we rewrite (10) as

$$p_N^d(s) = \int_0^s dl_2 \Psi_d(s - l_2, l_2) \quad \text{where} \quad (12)$$

$$\Psi_d(l_1, l_2) = N g^{N-1} \frac{\partial^2 g}{\partial l_1 \partial l_2} + N(N-1)g^{N-2} \frac{\partial g}{\partial l_1} \frac{\partial g}{\partial l_2}.$$

We interpret the two contributions in $\Psi_d(l_1, l_2)$ as follows [19]: the first term corresponds to a configuration where one particle explores a region $[-l_2, s - l_2]$ (we call it a box) of size s in unit time interval, such that its maximum is at $s - l_2$ and minimum is at $-l_2$, while all the other $(N - 1)$ particles stay inside this box. On the other hand, the second term corresponds to a configuration where two particles create, in a different way, the same box $[-l_2, s - l_2]$ of size s : one of the two particles has its maximum at $s - l_2$ and minimum larger than $-l_2$

while the second particle has its minimum at $-l_2$ and maximum below $s - l_2$ and all other $(N - 2)$ particles stay strictly inside this box.

When $s \rightarrow 0$ in (12), one can replace $g(l_1, l_2)$ (8) by its asymptotic behavior when $l_1, l_2 \rightarrow 0$ where $g(l_1, l_2) \sim \frac{4}{\pi} \sin\left(\frac{\pi l_2}{l_1 + l_2}\right) e^{-\frac{\pi^2}{4(l_1 + l_2)^2}}$. Inserting it in (12), we see that both terms in (12) contribute equally. After integration over l_2 , one then obtains the result announced in (4) for $s \rightarrow 0$ with $a_N = 4\pi^{3/2}N(N-1) \left(\frac{4}{\pi}\right)^{N-2} \frac{\Gamma(\frac{N-1}{2})}{\Gamma(\frac{N}{2})}$, where $\Gamma(x)$ is the Gamma function. To perform the large s asymptotic of $p_N^d(s)$ we use the Poisson summation formula: $g(l_1, l_2) = \sum_{m=0}^\infty (-1)^m [\text{erf}[m(l_1 + l_2) + l_1] + \text{erf}[m(l_1 + l_2) + l_2]]$. We use this form to evaluate the integrand in (12) in the limit $s \rightarrow \infty$. We see that the first term in (12), which corresponds to create a box $[-l_2, s - l_2]$ with one particle, decreases as $e^{-(s+l_2)^2} e^{-l_2^2}$ whereas the second term where the same box is created by two particles decreases as $e^{-(s-l_2)^2} e^{-l_2^2}$. Since l_2 is always +ve, the two particles term wins over the one particle term when $s \rightarrow \infty$: this is physically understandable because creating a very large span with two particles is more likely than creating the same one with a single particle. It also follows from this analysis that the integral over l_2 in (12) is dominated by $l_2 \sim \mathcal{O}(s)$, which yields finally the large s behavior announced in (4) with $b_N = 2N(N-1)/\sqrt{\pi}$. In Fig. 2 we verify that the small and large s asymptotics of $p_N^d(s)$ given in (4), for $N = 10$, describe very well, without any fitting parameter, the distribution obtained from direct simulation, without any fitting parameter.

What happens for large N ? The typical scale of the fluctuations of $S_N/\sqrt{2t}$ can be estimated from the relations with EVS (1). The variables \tilde{M}_i 's, with $i = 1, \dots, N$, which are the maxima of the i^{th} BM on the unit interval, are i.i.d. variables. Their common pdf is known to be a half-Gaussian, $p(M) = (2/\sqrt{\pi})e^{-M^2}$, $M > 0$. The same holds for the variables $-\tilde{m}_i$'s. Hence, for large N , standard results of EVS [25] state that the typical value of $\tilde{M}_+ = \max_{1 \leq i \leq N} \tilde{M}_i$ is $\mathcal{O}(\sqrt{\log N})$ while its fluctuations are of order $1/\sqrt{\log N}$ and governed by a Gumbel distribution. The same also holds for $\tilde{m}_- = -\min_{1 \leq i \leq N} \tilde{m}_i$. For large N , these two extremes become uncorrelated as the global maximum and global minimum are most likely reached by two independent walkers. Hence one gets

$$g^N \left[\mu_N + \frac{\tilde{l}_1}{2\mu_N}, \mu_N + \frac{\tilde{l}_2}{2\mu_N} \right] \xrightarrow{N \rightarrow +\infty} e^{-e^{-\tilde{l}_1}} e^{-e^{-\tilde{l}_2}} \quad (13)$$

with $\mu_N = \sqrt{\log N}$. Inserting (13) in (10) with $\tilde{s} = 2\mu_N(s - 2\mu_N)$ one finds

$$p_N^d(s) \sim 2\sqrt{\log N} \int_{-\infty}^\infty d\tilde{l}_2 e^{-\tilde{s}} e^{-e^{-\tilde{l}_2}} e^{-e^{-(\tilde{s}-\tilde{l}_2)}}, \quad (14)$$

which can be evaluated explicitly to give (6). In Fig. 2 we plot $p_N^d(s)/2\sqrt{\log N}$ against \tilde{s} for $N = 50$ and 100. They

show a relatively good agreement with the exact result $\mathcal{D}(\tilde{s})$ after an overall shift of order $\mathcal{O}(1/\log N)$ along the x -axis, thus revealing, as expected, a slow convergence towards the asymptotic result. In [14] the authors argued that the limiting distribution should be a Gumbel distribution, overlooking the fact that it is actually the *convolution* of two Gumbel distributions, as in (14). In particular, for large \tilde{s} , $\mathcal{D}(\tilde{s}) \sim \tilde{s}e^{-\tilde{s}}$, while the Gumbel distribution decays as a pure exponential.

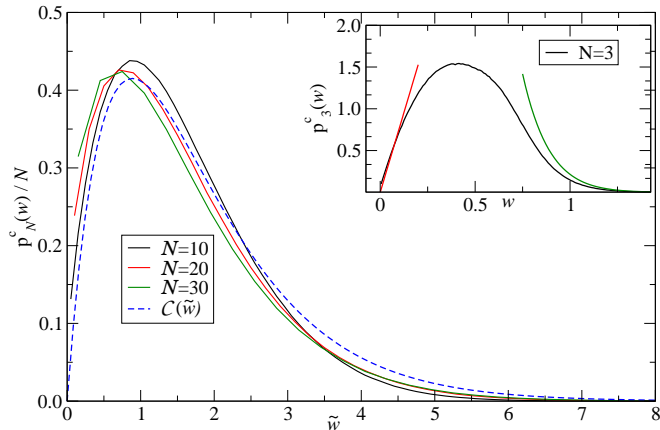


FIG. 3. (Color online) Plot of $p_N^c(w)/N$ as a function of $\tilde{w} = Nw$. The dotted line indicates the exact asymptotic results for $N \rightarrow \infty$, $\mathcal{C}(\tilde{w})$ in (7). **Inset:** Plot of $p_3^c(w)$, obtained from simulation, compared with its asymptotic behavior (5).

Common sites : To find the small and large w asymptotics of $P_N^c(w)$ we write (11) as

$$p_N^c(w) = \int_0^w dj_2 \Psi_c(w - j_2, j_2) \quad \text{where} \quad (15)$$

$$\Psi_c(j_1, j_2) = N h^{N-1} \frac{\partial^2 h}{\partial j_1 \partial j_2} + N(N-1) h^{N-2} \frac{\partial h}{\partial j_1} \frac{\partial h}{\partial j_2}.$$

In (15), one interprets the first term as one single particle creating a common span $[-j_2, w - j_2]$ of size w and the second term as two particles collaboratively creating the same common span (in a unit time interval) [19]. In both cases, the remaining particles are such that their maxima are above $w - j_2$ and their minima are below $-j_2$. When $w \rightarrow 0$ in (15), $h(j_1, j_2)$ can be replaced by its asymptotic behavior for small j_1, j_2 : $h(j_1, j_2) \sim \left(1 - \frac{2}{\sqrt{\pi}}(j_1 + j_2)\right)$. Integrating then over j_2 in (15) yields the small w behavior in (5) with $c_N = 4N(N-1)/\pi$. Note that for very small w , it is much more likely to create a box of size smaller than w with *two* particles (which occurs with a probability $\propto w^2$) than with a single one [which occurs with probability $\propto \exp(-\pi^2/4w^2)$]. The former configurations thus dominate for small w .

To get the large w behavior of $p_N^c(w)$, we estimate $h(j_1, j_2)$ for large j_1 (15). This is conveniently done by using the Poisson formula, which yields $h(j_1, j_2) \sim \text{erfc}(2j_1 + j_2) + \text{erfc}(j_1 + 2j_2)$. This estimate shows that

for $w \gg \sqrt{\log N}$, the second term in (15) becomes subdominant compared to the first one. Hence for very large w the leading contribution comes from the first term where we replace $h^{(N-1)}(w - j_2, j_2) \sim [\text{erfc}(w + j_2) + \text{erfc}(2w - j_2)]^{N-1}$ by $\text{erfc}^{(N-1)}(w)$ as one can show that the integral over j_2 in (15) is dominated by the vicinity of $j_2 = 0$ [19]. This leads to the large w behavior in (5) with $d_N = 8N/\pi^{N/2}$. The asymptotic behaviors of $p_N^c(w)$ (5) have been verified numerically for $N = 3$ in Fig. 3.

To obtain the typical scale of $W_N/\sqrt{2t}$ for large N , we use its relation to EVS (2). From standard EVS for i.i.d. random variables [25], we know that $\tilde{M}_- = \min_{1 \leq i \leq N} M_i$, where $M_i \geq 0$ and distributed according to a half-Gaussian, is of order $\mathcal{O}(N^{-1})$. Its pdf is given by a Weibull law, which is here an exponential distribution [25]. Indeed one has here $\text{Pr}.(N\tilde{M}_- \geq x) = e^{-\frac{2}{\sqrt{\pi}}x}$, $x > 0$, as $N \rightarrow \infty$. The same holds for \tilde{m}_+ , which for large N becomes independent of \tilde{M}_- as both of them are reached by two independent walkers. Hence, from (2), $NW_N/\sqrt{2t}$ is given by the convolution of two exponential laws:

$$p_N^c(w) \sim N^2(4/\pi)e^{-\frac{2}{\sqrt{\pi}}Nw} \int_0^w dk \sim N \mathcal{C}(Nw), \quad (16)$$

with $\mathcal{C}(\tilde{w})$ as announced in (7). We have also obtained this result [19] by a direct large N expansion of (15). In Fig. 3 we plot $p_N^c(w)/N$ against \tilde{w} for $N = 10, 20$ and 30 and see that they both coincide with the function $\mathcal{C}(\tilde{w})$, although the convergence is rather slow.

Conclusion : We have achieved a complete analytic description of the number of distinct and common sites visited by N independent RWs after t time steps, for large t . We have also obtained interesting limiting distributions (6, 7) in the limit when $N \rightarrow \infty$. For distinct sites, we found an intriguing connection with the maximum of logarithmically correlated random variables on a circle [20].

One may wonder about the effects of interactions between the walkers. For instance, one can study non-intersecting (vicious) RWs [27]. An interesting situation is the case where all N walkers start and end at the same point, while staying positive in the time interval $[0, t]$ (watermelons with a wall). In this case, the number of distinct sites $S_N/\sqrt{2t}$ corresponds to the maximal height of these watermelons [28]. For large N , the pdf of $S_N/\sqrt{2t} \propto \sqrt{N}$ properly shifted and scaled, converges to the Tracy-Widom distribution \mathcal{F}_1 [29], which describes the fluctuations of the largest eigenvalue of Gaussian orthogonal random matrices. On the other hand, the number of common sites $W_N/\sqrt{2t}$ is related to the maximum of the lower path, the distribution of which is a very interesting open problem [31].

We thank A. Perret for a useful discussion. This research was supported by ANR grant 2011-BS04-013-01 WALKMAT and in part by the Indo-French Centre

for the Promotion of Advanced Research under Project 4604 – 3.

-
- [1] R. J. Beeler and A. J. Delaney, Phys. Rev. A **130**, 962 (1963).
- [2] R. J. Beeler, Phys. Rev. A **134**, 1396 (1964).
- [3] A. Blumen, J. Klafter and G. Zumofen, in *Optical Spectroscopy of Glasses*, edited by I. Zschokke (Reidel, New York, 1986), pp. 199-265.
- [4] R. Czech, J. Chem. Phys. **91**, 2498 (1989).
- [5] P. Bordewijk, Chem. Phys. Lett. **32**, 592 (1975).
- [6] C. A. Condat, Phys. Rev. A **41**, 3365 (1990).
- [7] L. Edelstein-Keshet, *Mathematical Models in Biology* (Random House, New York, 1988).
- [8] E. C. Pielou, *An Introduction to Mathematical Ecology* (Wiley-Interscience, New York, 1969);
- [9] C. Cattuto, A. Barrat, A. Baldassari, G. Schehr and V. Loreto, Proc. Natl. Acad. Sci. USA **106**, 10511 (2009).
- [10] A. Dvoretzky and P. Erdős, in *Proceedings of the Second Berkeley Symposium on Mathematical Statistics and Probability* (University of California Press, Berkeley, 1951).
- [11] G. H. Vineyard, J. Math. Phys. **4**, 1191 (1963).
- [12] E. W. Montroll and G. H. Weiss, J. Math. Phys. **6**, 167 (1965).
- [13] F. van Wijland and H. J. Hilhorst, J. Stat. Phys. **89**, 119 (1997).
- [14] H. Larralde, P. Trunfino, S. Havlin, H. E. Stanley, and G. H. Weiss, Nature (London) **355**, 423 (1992); Phys. Rev. A **45**, 7128 (1992).
- [15] S. N. Majumdar and M. V. Tamm, Phys. Rev. E **86**, 021135 (2012).
- [16] L. Turban, preprint arXiv: 1209.2527
- [17] From now on, we drop the explicit t dependence on S_N, W_N, M_i, m_i .
- [18] with diffusion constant $D = 1/4$.
- [19] A. Kundu, S. N. Majumdar and G. Schehr, supplementary material.
- [20] Y. V. Fyodorov and J.-Ph. Bouchaud, J. Phys. A: Math. Theor. **41**, 372001 (2008).
- [21] D. Carpentier and P. Le Doussal, Phys. Rev. E **63**, 026110 (2001).
- [22] Y. V. Fyodorov, P. Le Doussal and A. Rosso, J. Stat. Mech., P10005 (2009).
- [23] M. Mézard, G. Parisi, M. Virasoro, *Spin-Glass Theory and Beyond*, (Singapore : World Scientific), (1997).
- [24] S. Redner, *A guide to first-passage processes*, Cambridge University Press, Cambridge, 2001.
- [25] E. J. Gumbel, *Statistics of Extremes*, Dover, (1958).
- [26] K. L. Chung, Ark. Mat. **14**(2), 155 (1976).
- [27] M. E. Fisher, J. Stat. Phys. **34**, 667 (1984).
- [28] G. Schehr, S. N. Majumdar, A. Comtet and J. Randon-Furling, Phys. Rev. Lett. **101**, 150601 (2008).
- [29] P. J. Forrester, S. N. Majumdar and G. Schehr, Nucl. Phys. B **844**, 500 (2011); Erratum Nucl. Phys. B **857**, 424 (2011).
- [30] C. A. Tracy and H. Widom, Commun. Math. Phys. **177**, 727 (1996).
- [31] C. A. Tracy and H. Widom, Ann. of App. Proba. **17** (3), 953 (2007).